

Slow light in saturable absorbers

Bruno Macke and Bernard Ségard*

Laboratoire de Physique des Lasers, Atomes et Molécules (PhLAM), Centre d'Etudes et de Recherches Lasers et Applications (CERLA), Université de Lille I, 59655 Villeneuve d'Ascq, France

(Received 5 February 2008; published 10 July 2008)

In connection with the experiments recently achieved on doped crystals, biological samples, doped optical fibers, and semiconductor heterostructures, we revisit the theory of the propagation of a pulse-modulated light in a saturable absorber. Explicit analytical expressions of the transmitted pulse are obtained, enabling us to determine the parameters optimizing the time-delay of the transmitted pulse with respect to the incident pulse. We finally compare the maximum fractional delay or figure of merit so attainable to those which have been actually demonstrated in the experiments.

DOI: [10.1103/PhysRevA.78.013817](https://doi.org/10.1103/PhysRevA.78.013817)

PACS number(s): 42.25.Hz, 42.25.Kb, 42.25.Lc

I. INTRODUCTION

Dynamics of saturable absorbers is often well reproduced by using a two-level model with a coherence relaxation time very short compared to the population relaxation time. The propagation of laser pulses in the medium is then simply described by two equations coupling the light intensity and the difference of populations. As far back as 1965, Gires and Combaud [1] used this model to analyze the transmission of laser pulses through dye solutions. They considered pulses of duration long compared to the population relaxation time, but this approximation is relaxed in subsequent works [2–5]. Calculations made by Selden in this more general case enabled him to explain not only the narrowing of the transmitted pulse but also its skewing and the time delay of its maximum [5]. Selden also studied the transmission of a laser beam when its intensity is slightly modulated by a low frequency sine wave [6]. He showed that the effect of the saturable absorber is to increase the modulation depth and to introduce a phase delay of this modulation. The experimental data obtained by Hillman *et al.* on ruby [7] are in full agreement with his predictions on the modulation depth. Although often overlooked, the above mentioned theories [2–6] are applicable to most of the recent experiments achieved on various saturable absorbers, including doped crystals [8–13], biological film and solution [14,15], quantum wells [16,17], quantum dots [18–20], and doped optical fibers [21,22]. Developed to attain pulse velocities as slow as possible, these experiments are currently analyzed in terms of coherent population oscillations (CPOs), homogeneous hole burning [23], and group velocity. As extensively discussed in Refs. [24–26], such an analysis is questionable. In most cases [27], the population oscillations are not created in the medium under the combined action of two independent coherent beams [23] but results from the intensity modulation of a single incident beam. The phenomenon is thus insensitive to phase and frequency fluctuations of the optical field. The group velocity, attached to a given optical frequency and obtained by expressing that the phase of the field is stationary near this frequency, then loses its relevance. We also

remark that the identification of the group velocity to the ratio of the medium thickness over the time-delay of the pulse maximum, often made in the literature, is incorrect. As a matter of fact, the saturable absorption and the CPO approaches are based on the same approximations, namely, that the coherence relaxation time is infinitely short compared to the population relaxation time, the Rabi period, and the inverse of the deviations of the laser frequency from the line frequency. In the CPO approach, analytical results have only been obtained in the particular case of a weak sine-wave modulation. The fact that the saturable absorption approach then gives exactly the same results [17,25,28] shows that the two approaches are equivalent. However, the saturable absorption approach is more straightforward (it avoids the passage through the refractive index) and, as shown in the following, is more efficient since it provides analytical results in much more general situations, in particular, not only when the pulse acts as a probe but also when its interaction with the medium is fully nonlinear. Finally the saturable absorption approach better corresponds to the experimental conditions where the inverse of the pulse duration is generally much smaller than the fluctuations of the optical carrier frequency.

For the first time to our knowledge, we provide in the present paper explicit analytical expressions of the transmitted pulse with a special attention paid to its delay with respect to the incident pulse and to the optimization of this delay. In Sec. II, we recall the general equations describing the propagation of intensity-modulated light in a saturable absorber. The case of pulses superimposed to a continuous background with a small modulation index is examined in Sec. III. The nonlinear propagation of pulses in the absence of background and the general case (pulses and background of arbitrary intensity) are respectively studied in Secs. IV and V. We finally compare in Sec. VI the fractional delays attainable with saturable absorbers to those which have been actually demonstrated.

II. GENERAL ANALYSIS

We consider a resonant light beam propagating in the z direction through a saturable absorber modeled as a two-level system. As indicated before, we assume that the coher-

*bernard.segard@univ-lille1.fr

ence relaxation time is infinitely short compared to the population relaxation time, the Rabi period, and the inverse of the deviations of the laser frequency from the line frequency. It is then possible to adiabatically eliminate the polarization in the Bloch-Maxwell equations in order to obtain the two coupled equations [1–4]

$$\tau \frac{\partial N}{\partial t} = N(1 + I) - 1, \quad (1)$$

$$\frac{\partial I}{\partial z} = -\alpha I N. \quad (2)$$

In these expressions, τ is the population relaxation time, N is the population difference normalized to its value at equilibrium, t is the time retarded by the propagation time in the host medium (negligible compared to the delays considered in the following), I is the beam intensity normalized to the saturation intensity [29], and α is the absorption coefficient in the linear regime. Combining Eqs. (1) and (2) we easily get the nonlinear wave equation

$$\frac{\partial}{\partial z} \left(\tau \frac{\partial I}{\partial t} + I + \ln I + \alpha z \right) = 0 \quad (3)$$

and the transmission equation

$$\tau \frac{\partial I_{\text{out}}}{\partial t} + I_{\text{out}} + \ln I_{\text{out}} + \alpha L = \tau \frac{\partial I_{\text{in}}}{\partial t} + I_{\text{in}} + \ln I_{\text{in}}, \quad (4)$$

where L is the absorber thickness and I_{out} (I_{in}) is the normalized intensity of the output (input) wave. When the input intensity is constant or very slowly varying at the scale of τ , Eq. (4) is reduced to the well-known saturation equation [2–4,7]

$$I_{\text{out}} + \ln I_{\text{out}} + \alpha L = I_{\text{in}} + \ln I_{\text{in}}. \quad (5)$$

Although established with a two level model, this equation fits very well the transmission curve of multilevel saturable absorbers. This result is illustrated Fig. 1, where we compare the predicted transmission to that actually measured on a erbium-doped optical fiber [30].

III. CASE OF SMALL MODULATION INDEX

We consider first the important case where the pulses (containing the useful signal) are superimposed to a large dc background C . The input and output intensities, respectively, read $I_{\text{in}}(t) = C_{\text{in}} + s_{\text{in}}(t)$ with $s_{\text{in}}(t) \ll C_{\text{in}}$ and $I_{\text{out}}(t) = C_{\text{out}} + s_{\text{out}}(t)$ with $s_{\text{out}}(t) \ll C_{\text{out}}$. Making a calculation at the first order in $s_{\text{in}}(t)$ and $s_{\text{out}}(t)$ and taking into account Eq. (5) relating C_{out} and C_{in} , we get

$$\frac{ds_{\text{out}}}{dt} + \frac{s_{\text{out}}}{\tau_b} = \frac{C_{\text{out}}}{C_{\text{in}}} \left(\frac{ds_{\text{in}}}{dt} + \frac{s_{\text{in}}}{\tau_a} \right), \quad (6)$$

where $\tau_a = 1/(1 + C_{\text{in}})$ and $\tau_b = 1/(1 + C_{\text{out}})$. Assuming that $s_{\text{in}}(-\infty) = 0$, the general solution of Eq. (6) may be written

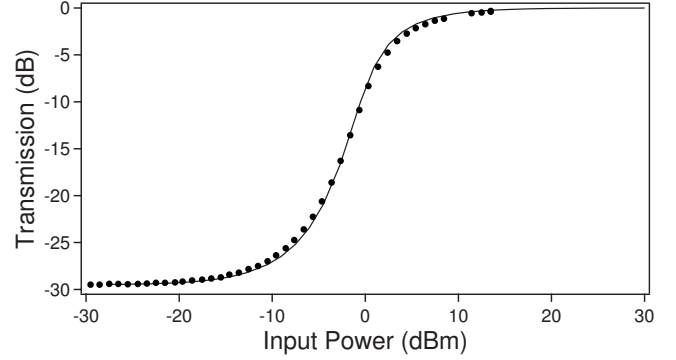


FIG. 1. Transmission at 1530 nm of an erbium-doped optical fiber as a function of the incident power. The parameters are $L = 7.5$ m and $\alpha L = 6.8$. The points are experimental [30] and the continuous line is obtained from Eq. (5) by adjusting the saturation power P_{sat} . The best fit is obtained for $P_{\text{sat}} = -7.30$ dBm, that is, $P_{\text{sat}} = 0.186$ mW. The erbium concentration is small enough in order that energy transfer up-conversion is negligible and that the absorption is fully saturable.

$$s_{\text{out}}(t) = \frac{C_{\text{out}}}{C_{\text{in}}} \left[s_{\text{in}}(t) + \left(\frac{1}{\tau_a} - \frac{1}{\tau_b} \right) e^{-t/\tau_b} \int_{-\infty}^t s_{\text{in}}(\theta) e^{\theta/\tau_b} d\theta \right]. \quad (7)$$

The impulse response $h(t)$ [31] is obtained by taking $s_{\text{in}}(t) = \delta(t)$ where $\delta(t)$ is the Dirac function. We get

$$h(t) = \frac{C_{\text{out}}}{C_{\text{in}}} \left[\delta(t) + \left(\frac{\tau_b - \tau_a}{\tau_a} \right) \frac{U(t)}{\tau_b} e^{-t/\tau_b} \right], \quad (8)$$

where $U(t)$ is the unit step function. Finally the transfer function [31], Fourier transform of $h(t)$, reads

$$H(\Omega) = \frac{C_{\text{out}}}{C_{\text{in}}} \left(1 + \frac{\tau_b - \tau_a}{\tau_a(1 + i\Omega\tau_b)} \right) \equiv \frac{C_{\text{out}}\tau_b(1 + i\Omega\tau_a)}{C_{\text{in}}\tau_a(1 + i\Omega\tau_b)}. \quad (9)$$

The latter result can also be directly derived from Eq. (6) by taking $s_{\text{in}}(t) \propto e^{i\Omega t}$ [25] and is obviously applicable to the particular case of a sine-wave modulation, often used in the experiments. It is consistent with the previous calculations made in this case [6,8,25] and with the experimental results. The phase delay of the intensity modulation introduced by the medium has a maximum $\Delta\Phi_m = \tan^{-1}[(\tau_a - \tau_b)/2\sqrt{\tau_a\tau_b}]$ for $\Omega = 1/\sqrt{\tau_a\tau_b}$. We remark that $\Delta\Phi_m < \pi/2$, the upper limit being approached for $C_{\text{in}} \gg 1$ and $C_{\text{out}} \ll 1$. Consequently the time delay t_d of the output modulation can never exceed 25% of the modulation period T .

Strictly speaking a sine wave does not contain any information and, e.g., the previous delay t_d may also be seen as an advance $T - t_d$. An unambiguous demonstration of delay (or advance) requires to use pulses of finite duration and energy. Ultraslow “velocities” L/t_d can be achieved by using dense media with long relaxation times [14,15]. However, in view of potential applications, the important issue is not merely to achieve ultraslow light but to produce delays as large as possible compared to the duration of both the input and the

output pulses. In the following we will thus characterize the slow light systems by their figure of merit or generalized fractional delay

$$F = t_d / \max(\tau_{\text{in}}, \tau_{\text{out}}), \quad (10)$$

where τ_{in} (τ_{out}) is the full width at half maximum of the input (output) pulse. Our definition is identical to the usual one ($F = t_d / \tau_{\text{in}}$) when $\tau_{\text{out}} \approx \tau_{\text{in}}$ or $\tau_{\text{out}} < \tau_{\text{in}}$.

We consider input pulses such that $s_{\text{in}}(t)$ is continuous, bell-shaped, symmetric, and centered at $t=0$. General properties of the output pulse $s_{\text{out}}(t)$ can be derived from the relations $s_{\text{out}}(t) = h(t) \otimes s_{\text{in}}(t)$ or $S_{\text{out}}(\Omega) = H(\Omega)S_{\text{in}}(\Omega)$, where $S_{\text{out}}(\Omega)$ and $S_{\text{in}}(\Omega)$ are, respectively, the Fourier transforms of $s_{\text{out}}(t)$ and $s_{\text{in}}(t)$. Since $s_{\text{in}}(t)$ is centered at $t=0$, the center-of-mass $t_{\text{c.m.}}$ of $s_{\text{out}}(t)$ coincides with that of $h(t)$. We get

$$t_{\text{c.m.}} = \frac{\int_{-\infty}^{+\infty} th(t)dt}{\int_{-\infty}^{+\infty} h(t)dt} = \tau_b - \tau_a. \quad (11)$$

Since $\tau_a = \tau / (1 + C_{\text{in}})$ and $\tau_b = \tau / (1 + C_{\text{out}})$, $t_{\text{c.m.}}$ will be always smaller than the relaxation time τ , this limit being only attained when $C_{\text{in}} \gg 1$ and $C_{\text{out}} \ll 1$. The largest pulse delays are expected in these conditions but one should remark that, due to the distortion (asymmetric broadening), the delay t_d of the pulse maximum may strongly differ from $t_{\text{c.m.}}$. Equations (7) and (8) show that the distortion will be negligible when $\tau_{\text{in}} \gg \tau_b$ (long pulses). We have then $t_d \approx t_{\text{c.m.}}$ and thus $F \ll 1$. More generally t_d will be as large as possible if the first term of Eq. (7) (not delayed) is small compared to the second one, that is again when $C_{\text{in}} \gg 1$, $C_{\text{out}} \ll 1$, and thus $t_{\text{c.m.}} \approx \tau$. We then get $s_{\text{out}}(t) \approx C_{\text{out}}g(t)$ with

$$g(t) = \left[\frac{U(t)}{\tau} e^{-t/\tau} \right] \otimes s_{\text{in}}(t) = \frac{e^{-t/\tau}}{\tau} \int_{-\infty}^t s_{\text{in}}(\theta) e^{\theta/\tau} d\theta \\ = \mathcal{T}^{-1} \left[\frac{S_{\text{in}}(\Omega)}{1 + i\Omega\tau} \right], \quad (12)$$

where \mathcal{T}^{-1} is a shorthand notation of the inverse Fourier transform. When $\tau_{\text{in}} \ll \tau$ (short pulses), Eq. (12) shows that $t_d = O(\tau_{\text{in}})$ while $\tau_{\text{out}} \approx \tau \ln 2$ [the duration of $U(t)e^{-t/\tau}$] and thus $F \ll 1$, as previously. A maximum of the fractional delay is expected for $\tau_{\text{in}} = O(\tau)$ but its determination obviously requires to specify the pulse shape.

We consider first the realistic case of pulses having a strictly finite duration (hereafter cos pulses), such that $s_{\text{in}}(t) = A_{\text{in}} \cos^2(\pi t / 2\tau_{\text{in}})$ for $-\tau_{\text{in}} \leq t \leq \tau_{\text{in}}$ and $s_{\text{in}}(t) = 0$ elsewhere (Fig. 2). Equation (12) then leads to

$$g(t) \approx \frac{A_{\text{in}}}{2} \left[1 + \frac{\cos\left(\frac{\pi t}{\tau_{\text{in}}}\right) + \frac{\pi t}{\tau_{\text{in}}} \sin\left(\frac{\pi t}{\tau_{\text{in}}}\right) - \left(\frac{\pi t}{\tau_{\text{in}}}\right)^2 e^{-(t+\tau_{\text{in}})/\tau}}{(\pi t / \tau_{\text{in}})^2 + 1} \right] \quad (13)$$

for $-\tau_{\text{in}} \leq t \leq \tau_{\text{in}}$, $g(t < -\tau_{\text{in}}) = 0$ and $g(t > \tau_{\text{in}}) = g(\tau_{\text{in}})e^{-(t-\tau_{\text{in}})/\tau}$. As expected, $s_{\text{out}}(t)$ has an exponential fall at the end of the input pulse ($t > \tau_{\text{in}}$). The time delay t_d of the maximum is given by the implicit equation

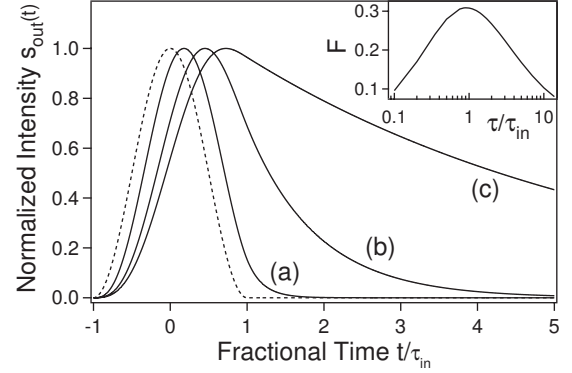


FIG. 2. Intensity profile of the output pulses obtained in the case of small modulation index for τ / τ_{in} : (a) 0.2, (b) 0.9, and (c) 5. The profile of the input pulse (cos pulse) is given for reference (dashed line). The time unit is its full width at half maximum τ_{in} . Inset: Fractional delay as a function of the ratio τ / τ_{in} .

$$\sin\left(\frac{\pi t_d}{\tau_{\text{in}}}\right) = \left(\frac{\pi \tau}{\tau_{\text{in}}}\right) \left[\cos\left(\frac{\pi t_d}{\tau_{\text{in}}}\right) + e^{-(t_d + \tau_{\text{in}})/\tau} \right]. \quad (14)$$

Asymptotic calculations show that $t_d \approx \tau(1 - \pi^2 \tau^2 / 2\tau_{\text{in}}^2)$ for $\tau_{\text{in}} \gg \tau$ and that $t_d \approx \tau_{\text{in}}(1 - 2\tau_{\text{in}}^{1/2} / \pi\tau^{1/2})$ for $\tau_{\text{in}} \leq \tau$. When τ / τ_{in} varies from 0 to ∞ , t_d / τ_{in} increases from 0 to 1 while τ_{out} increases from τ_{in} to ∞ ($\tau_{\text{out}} \approx \tau \ln 2$, see above). Starting from 0, the fractional delay F , equal here to t_d / τ_{out} , begins to increase before to decrease to 0, in agreement with our general predictions (see inset of Fig. 2). It attains its maximum $F_{\text{max}} = 31\%$ for $\tau / \tau_{\text{in}} = 0.9$. This maximum is very flat since $F_{\text{max}} > 29\%$ for $0.6 < \tau / \tau_{\text{in}} < 1.5$. Figure 2 shows the intensity profiles of the output pulses obtained for $\tau / \tau_{\text{in}} = 0.2, 0.9$, and 5.

Similar results are obtained in the classical case of Gaussian pulses. Taking $s_{\text{in}}(t) = A_{\text{in}} \exp(-t^2 / \tau_p^2)$ with $\tau_p = \tau_{\text{in}} / 2\sqrt{\ln 2}$, we get

$$g(t) \approx A_{\text{in}} \frac{\tau_p \sqrt{\pi}}{2\tau} \left[1 + \text{erf}\left(\frac{t}{\tau_p} - \frac{\tau_p}{2\tau}\right) \exp\left(-\frac{t}{\tau} + \frac{\tau_p^2}{4\tau^2}\right) \right], \quad (15)$$

where $\text{erf}(x)$ is the error function. The optimal τ / τ_{in} (1.05) is close to that obtained with cos pulses and F_{max} is nearly the same (29%). The main difference is that the delay t_d is no longer limited by τ_{in} . Delays $t_d \geq \tau_{\text{in}}$ can be obtained when $\tau / \tau_{\text{in}} \gg 1$. Asymptotic calculations then show that $t_d = \tau_p [\ln(\frac{\tau}{\tau_p \pi})]^{1/2}$. A delay $t_d \approx \tau_{\text{in}}$ is attained for $\tau / \tau_{\text{in}} \approx 17$. The output pulse is then very broad ($\tau_{\text{out}} \approx 12\tau_{\text{in}}$ and $F \approx 8\%$). When the double condition $C_{\text{in}} \gg 1$ and $C_{\text{out}} \ll 1$ is not met, the term proportional to $s_{\text{in}}(t)$ in $s_{\text{out}}(t)$ [see Eq. (7)] is not negligible and $\tau_b < \tau$. The fractional delay is reduced accordingly. Considering, e.g., cos pulses with $C_{\text{in}} = 1$ and $C_{\text{out}} = 1/10$ (attained by taking $\alpha L \approx 3.2$), we find $F_{\text{max}} \approx 9\%$ instead of 31% in the ideal case.

IV. PULSES WITHOUT BACKGROUND

We consider now the case where $C_{\text{in}} = 0$, without restriction on the pulse amplitude. The medium being initially at

equilibrium [$N(-\infty)=1$], Eqs. (1) and (2) show that $N(t) > 0$ and $s_{\text{out}}(t) < s_{\text{in}}(t)$ at every time. If the input pulse has a strictly finite duration (as the cos pulses), $s_{\text{out}}(t)$ will thus stop at the same time that $s_{\text{in}}(t)$. This result strongly contrasts with that obtained in the previous section (see Fig. 2).

When the input pulse is very short ($\tau_{\text{in}} \ll \tau$), the population difference cannot follow the rapid change of the intensity and, roughly speaking, retains its initial value (sudden approximation). From Eq. (2), we then retrieve the result corresponding to the linear regime, namely, $s_{\text{out}}(t) = \exp(-\alpha L)s_{\text{in}}(t)$. The pulse is only attenuated (neither distorted nor delayed). Conversely, when the input pulse is very long, $s_{\text{out}}(t)$ and $s_{\text{in}}(t)$ are related by Eq. (5). The output pulse remains symmetric and centered at $t=0$ (no delay) but may be strongly narrowed [5]. Finally, when τ_{in} and τ are comparable, the output pulse will be at once narrowed, delayed and skewed. To study the general case, we consider the function $Z(t)$ introduced by Selden [4]:

$$Z(t) = \ln s_{\text{out}}(t) - \ln s_{\text{in}}(t) + \alpha L. \quad (16)$$

The transmission equation (4) then reads

$$\tau \frac{dZ}{dt} + Z = s_{\text{in}}(t)[1 + e^{(Z-\alpha L)}] = s_{\text{in}}(t) - s_{\text{out}}(t) \quad (17)$$

with the initial condition $Z(-\infty)=0$. For given $s_{\text{in}}(t)$, Eq. (17) shows that $Z(t)$ and thus the shape of the output pulse will be independent of the optical thickness αL as early as the latter is large enough in order that $s_{\text{out}}(t) \ll 1$ and $s_{\text{out}}(t) \ll s_{\text{in}}(t)$ at every time. The pulse delay is expected to have then attained its maximum. We have checked this point by numerically solving Eq. (17). Since we are mainly interested in maximizing the fractional delay, we will assume in the following that the previous condition on αL is actually met. Equation (17) is then reduced to

$$\tau \frac{dZ}{dt} + Z = s_{\text{in}}(t) \quad (18)$$

with the analytical solutions

$$Z(t) = \frac{e^{-t/\tau}}{\tau} \int_{-\infty}^t s_{\text{in}}(\theta) e^{-\theta/\tau} d\theta, \quad (19)$$

$$s_{\text{out}}(t) = e^{-\alpha L} s_{\text{in}}(t) e^{Z(t)}. \quad (20)$$

We see that $Z(t)=g(t)$, where $g(t)$ is the function introduced in Sec. III [Eqs. (12), (13), and (15)]. Consequently the delays t_d considered in Sec. III are now the delays t_Z of the maximum of $Z(t)$ and thus of $s_{\text{out}}(t)/s_{\text{in}}(t)$. Moreover, $s_{\text{in}}(t)$ being centered at $t=0$, Eq. (20) shows that the new delay t_d of the pulse maximum will be smaller than t_Z and that, for an input pulse of given shape, t_d (τ_{out}) will be the larger (smaller), the larger is the amplitude A_{in} .

For a given amplitude A_{in} , the shape of the output pulse and the fractional delay $F=t_d/\tau_{\text{in}}$ only depends on the ratio τ/τ_{in} . For long pulses ($\tau_{\text{in}} \gg \tau$), Eq. (18) takes the approximate form $Z(t+\tau) \approx s_{\text{in}}(t)$. We then get $t_Z \approx \tau$, $s_{\text{out}}(t) \approx e^{-\alpha L} s_{\text{in}}(t) \exp[s_{\text{in}}(t-\tau)]$ and, since $ds_{\text{in}}/dt=0$ for $t=0$, $t_d/\tau \approx A_{\text{in}}/(A_{\text{in}}+1)$. For $\tau/\tau_{\text{in}} \rightarrow 0$, $F \rightarrow 0$ as expected and $s_{\text{out}}(t)$ tends to the value given by Eq. (5) so long as αL is actually

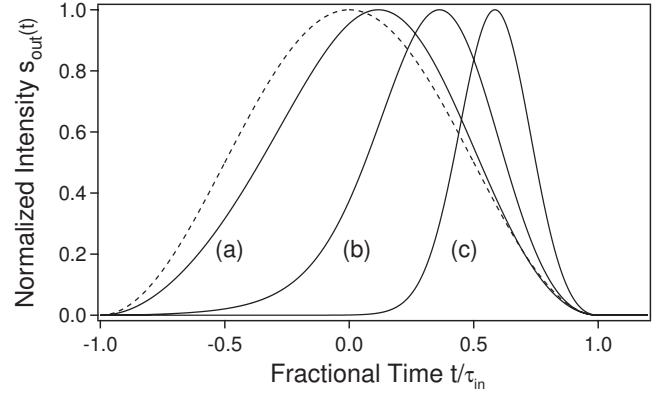


FIG. 3. Intensity profile of the output pulses obtained in the case of an input pulse without background for A_{in} : (a) 1, (b) 10, and (c) 100 with $\tau/\tau_{\text{in}} =$ (a) 0.6, (b) 1.5, and (c) 4.2 (the value maximizing the fractional delay in each case). The profile of the input pulse (cos pulse) is given for reference (dashed line).

large enough in order that $s_{\text{out}}(t) \ll 1$. Conversely when $\tau/\tau_{\text{in}} \rightarrow \infty$, $dZ/dt \rightarrow 0$, $Z(t) \rightarrow Z(-\infty)=0$, $s_{\text{out}}(t) \rightarrow e^{-\alpha L} s_{\text{in}}(t)$ (as in the general case) and, again, $F \rightarrow 0$. Finally, a maximum of F (increasing function of A_{in}) will be obtained for an intermediate value of τ/τ_{in} .

Figure 3 shows the intensity-profiles of the output pulse obtained with cos pulses for $A_{\text{in}}=1, 10$, and 100 (keep in mind that A_{in} is the peak intensity of the input pulse normalized to the saturation intensity). For each A_{in} , τ/τ_{in} is optimized in order to lead F to its maximum F_{max} . Note that the narrowing of the output pulses is significant but that their skewing is moderate (fall steeper than the rise). We have systematically explored how F_{max} , the corresponding $\tau_{\text{out}}/\tau_{\text{in}}$ and t_Z/τ_{in} depend on the saturation for A_{in} ranging from 0.2 to 10000 (Fig. 4). Since $s_{\text{in}}(t)$ stops at $t=\tau_{\text{in}}$, the fractional delay cannot exceed unity. In fact, the limit $F_{\text{max}}=1$ is very slowly approached for very large values of A_{in} . Asymptotic calculations then show that $F_{\text{max}} \approx 1 - (128/\pi^4 A_{\text{in}})^{1/5}$, this maximum being attained for $\tau/\tau_{\text{in}} \approx (2A_{\text{in}}^2/\pi^2)^{1/5}$. Even for A_{in} as large as 10000, F_{max} is only 0.83.

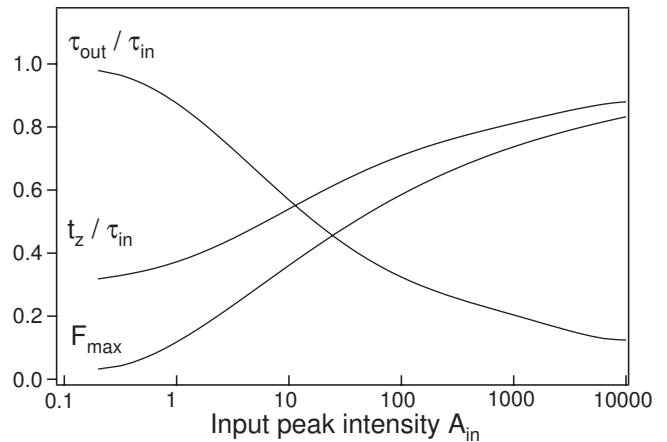


FIG. 4. F_{max} , t_Z/τ_{in} , and $\tau_{\text{out}}/\tau_{\text{in}}$ as functions of the peak intensity A_{in} in the case of cos pulses. For $A_{\text{in}} \geq 1000$, the ratio τ/τ_{in} maximizing F and F_{max} itself are well approximated by the asymptotic formula $\tau/\tau_{\text{in}} \approx (2A_{\text{in}}^2/\pi^2)^{1/5}$ and $F_{\text{max}} \approx 1 - (128/\pi^4 A_{\text{in}})^{1/5}$.

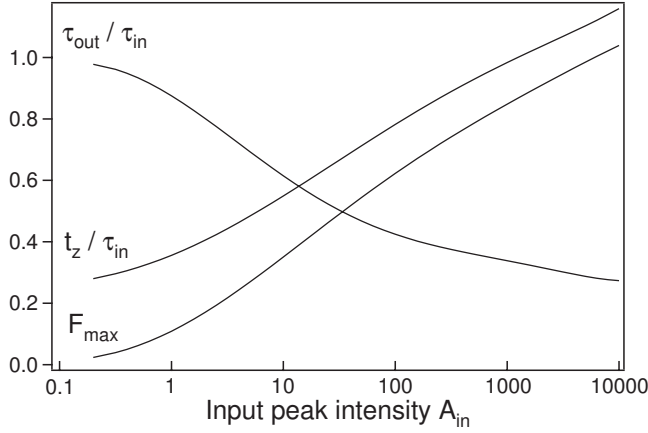


FIG. 5. Same as Fig. 4 in the case of Gaussian pulses. The ratio τ/τ_{in} maximizing F is 0.6, 1.5, 5.0, 14, and 42, respectively, for $A_{in}=1, 10, 100, 1000,$ and 10000 .

Comparable results are obtained with Gaussian pulses for reasonable peak intensities of the input pulse, say for $A_{in} \leq 50$ (Fig. 5). For larger A_{in} , some differences appear because the Gaussian pulses have infinite wings. There is thus no theoretical limit to t_z and t_d . For example, F_{max} slightly larger than 1 is attained for $A_{in}=10000$.

At this point, one should recall that the previous fractional delays F_{max} will be actually attained only if the optical thickness is large enough in order that $s_{out}(t) \ll s_{in}(t)$ at every time, that is if $\exp[Z_{max} - \alpha L] \ll 1$ where $Z_{max} = Z(t_z)$. This condition is satisfactorily met for $\alpha L = Z_{max} + 3$. When A_{in} is small (large), the optimum τ/τ_{in} is also small (large). In the first case $Z(t+\tau) \approx s_{in}(t)$ (see above) and $Z_{max} \approx A_{in} \ll 1$. In the second one, we easily get the asymptotic forms $Z_{max} \approx r A_{in} \tau_{in} / \tau$ with $r=1$ for cos pulses and $r = \sqrt{\pi}/2 \sqrt{\ln 2} \approx 1.06$ for Gaussian pulses ($1 \ll Z_{max} \ll A_{in}$). For intermediate values of A_{in} , $Z_{max} \leq \min(A_{in}, r A_{in} \tau_{in} / \tau)$ and the condition $s_{out}(t) \ll s_{in}(t)$ will be met in every case by taking

$$\alpha L = \min(A_{in}, r A_{in} \tau_{in} / \tau) + 3. \quad (21)$$

Provided that τ/τ_{in} is actually optimized to attain F_{max} , the second condition of validity of our calculation, namely, $s_{out}(t) \ll 1$, is then automatically fulfilled.

V. PULSE AND BACKGROUND OF ARBITRARY INTENSITY

Comparing the results obtained with input pulses superimposed to a large background (Sec. III) and with pulses without background (Sec. IV), we see that the former are broadened in the medium with a rise significantly steeper than the fall (Fig. 2) whereas the latter are narrowed with a fall steeper than the rise (Fig. 3). We may then hope that better results will be obtained by using pulses superimposed to a suitably adjusted background. We thus consider in this section the case where $I_{in}(t) = C_{in} + s_{in}(t)$ without restriction on the amplitudes of C_{in} and $s_{in}(t)$. As previously and for the same reasons, we assume that αL is large enough in order that $I_{out}(t) \ll 1$ and $I_{out}(t) \ll I_{in}(t)$ at every time. By redefining $Z(t)$ as $Z(t) = \ln I_{out}(t) - \ln I_{in}(t) + \alpha L - C_{in}$, we find that Eq.

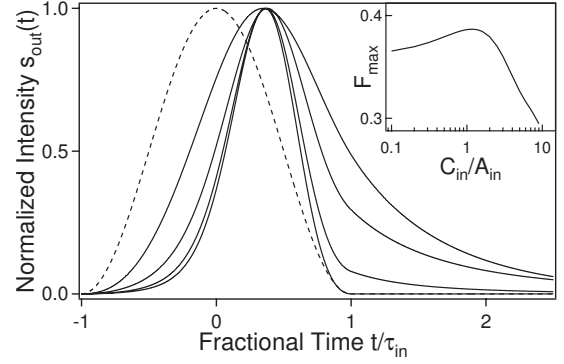


FIG. 6. Intensity profile of the output pulses obtained for an overall peak intensity $A_{in} + C_{in} = 10$. In order of increasing width, the represented profiles correspond to $C_{in}/A_{in} = 0, 0.11, 0.54,$ and 9.0 . For each value of C_{in}/A_{in} , τ/τ_{in} is optimized in order to maximize the fractional delay. The profile of the input pulse (cos pulse) is given for reference (dashed line). Inset: F_{max} as a function of C_{in}/A_{in} .

(18) is unchanged and thus that $Z(t) = g(t)$ as previously. In other respects the new definition of $Z(t)$ leads to

$$C_{out} + s_{out}(t) = [C_{in} + s_{in}(t)] e^{[C_{in} + g(t) - \alpha L]}. \quad (22)$$

Since $s_{in}(t)$, $s_{out}(t)$, and $g(t)$ cancel for $t = \pm \infty$, $C_{out} = C_{in} \exp(C_{in} - \alpha L)$ in agreement with Eq. (5) in the limit $C_{out} \ll 1$ considered here. Finally $s_{out}(t)$ reads

$$s_{out}(t) = [C_{in}(e^{g(t)} - 1) + s_{in}(t)e^{g(t)}] e^{(C_{in} + \alpha L)}. \quad (23)$$

When $C_{in} = 0$, we retrieve the result given in the previous section [Eq. (20)]. Conversely when the modulation index is small, $e^{g(t)} - 1 \approx g(t)$ and we get

$$s_{out}(t) = [s_{in}(t) + C_{in}g(t)] \frac{C_{out}}{C_{in}} \quad (24)$$

a result consistent with Eq. (7), again in the limit $C_{out} \ll 1$ where $\tau_b \approx \tau$.

Equation (23) enables us to determine the profiles of the output pulses for arbitrary values of the ratio C_{in}/A_{in} . We give Fig. 6 different profiles obtained when the input peak-intensity is fixed ($C_{in} + A_{in} = 10$). For each value of C_{in}/A_{in} , τ/τ_{in} has been optimized in order to maximize F . As expected the addition of a background widens the output pulse. It does not significantly enlarge the attainable fractional delay, which very slightly increases as a function of C_{in}/A_{in} before falling down to the value calculated in the small modulation-index limit (see inset of Fig. 6). However, we remark that the resemblance of the output pulse to the input one can be improved by the presence of a background (see the profile of the output pulse obtained for $C_{in}/A_{in} = 0.54$). The latter effect has been recently demonstrated in a saturable gain system [32]. The qualitative behavior shown Fig. 6 is general and is observed for any bell-shaped input pulse.

VI. SUMMARY AND DISCUSSION

We have theoretically studied the transmission of a pulse-modulated light in a saturable medium modeled as an en-

semble of two-level atoms with a coherence relaxation time extremely short compared to the population relaxation time. This model of saturable absorber gives theoretical results in good agreement with the experimental results obtained in the currently called CPO based slow light experiments. This was already pointed out in Ref. [25] about the representative experiments achieved on ruby [8], $\text{Er}^{3+}:\text{Y}_2\text{SiO}_5$ crystal [13], biological bacteriorhodopsin [14], and quantum dots [18]. We checked that it is also true for the extensive experiments recently realized on erbium-doped optical fibers [22]. More specifically, we verified that, except for ultrahighly doped fibers (ion density exceeding $3 \times 10^{25} \text{ m}^{-3}$), the maximum phase delays $\Delta\Phi_m$ attained for a sine-wave modulation and the corresponding modulation frequency are in agreement with those given by the model [see the discussion following Eq. (9)].

Thanks to the relative simplicity of the transmission equation of the model system [Eq. (4)], it has been possible to obtain explicit analytical expressions of the output pulse and to optimize the figure of merit or fractional delay F of the system [Eq. (10)]. Our main findings are as follows. When the input pulse sits on a much larger dc background C_{in} (intensity normalized to the saturation intensity), the output pulse is asymmetrically widened with a rise steeper than the fall. This behavior is qualitatively analog to that of the usual slow light systems (see, e.g., Ref. [33]) but the pulse shape may be much more asymmetric, with an exponential or nearly exponential fall (Fig. 2). The fractional delay F depends on C_{in} , on the linear optical thickness αL (which determines the intensity of the output dc background C_{out}) and on the ratio τ/τ_{in} of the population relaxation time over the width of the incident pulse. It attains its maximum $F_{\text{max}} \approx 30\%$ (slightly depending on the precise shape of the input pulse) when $C_{\text{in}} \gg 1$, $C_{\text{out}} \ll 1$, and $\tau/\tau_{\text{in}} \approx 1$. When $C_{\text{in}} = 1$ and $C_{\text{out}} = 1/10$ ($\alpha L \approx 3.2$), F_{max} falls down to 9%. Larger fractional delays are obtained by using input pulses of large peak intensity A_{in} without background. Contrary to the previous case the output pulse is now narrowed with a fall moderately steeper than the rise (Fig. 3). The largest fractional delays are attained when A_{in} is as large as possible (Figs. 4 and 5) provided that the optical thickness is itself very large [Eq. (21)]. Note that the ratio τ/τ_{in} maximizing F also increases with A_{in} . In the reference case $A_{\text{in}} = 10$, $F_{\text{max}} \approx 36\%$ for $\tau/\tau_{\text{in}} \approx 1.5$ and $\alpha L \approx 10.7$ [34]. Finally, for a fixed value of

the overall peak intensity of the input beam, the addition of a dc background does not significantly enhance the fractional delay but may improve the symmetry of the output pulse (Fig. 6).

In fact, there are few time-resolved experiments on saturable absorbers giving direct evidence of pulse delays [8,10,12,18,21,22]. The obtained fractional delays [as defined Eq. (10)] are all smaller than 20%. There are different reasons for that. The main one is that the input intensities C_{in} and/or A_{in} are too small, typically of the order of 1, at the best of a few units. Second the linear optical thickness is not adapted. Third the pulse duration is not optimized. The erbium-doped optical fiber seems a good candidate for the demonstration of a larger fractional delay. The saturation power is low ($< 0.5 \text{ mW}$) and normalized intensities C_{in} and/or A_{in} of 100 can be easily achieved. A fractional delay of about 60% [Fig. 3(c)] would then be attained with an input pulse of duration $\tau_{\text{in}} \approx 0.23\tau \approx 2.4 \text{ ms}$ and a linear optical thickness $\alpha L \approx 23$. The latter would be obtained in a fiber of reasonable length ($L < 4 \text{ m}$) with an ion density $\rho \approx 2 \times 10^{25} \text{ m}^{-3}$ [22] for which the saturation model is valid. Note that larger fractional delays (up to 1.5 with our definition) have been demonstrated in undoped fibers by exploiting Brillouin scattering [35] but this result is obtained with much longer fibers.

We finally remark that the pulse-delay mechanisms in a saturable absorber strongly differ from those involved in the “pure” slow-light experiments [36]. The former are nonlinear and non coherent whereas the latter are linear and coherent. Moreover the propagation phenomena are essential in the second case whereas they are absent in the first one. This point is illustrated by our calculations made for an input pulse of strictly finite duration (Sec. IV). We have shown that the output pulse then stops at the same time as the input one. On the contrary the propagation effects are responsible of an important delay in the linear case. This explains in particular the very large fractional delays attained in media with an electromagnetically induced [37] or a natural [38,39] transparency window.

ACKNOWLEDGMENTS

Laboratoire PhLAM is Unité Mixte de Recherche de l’Université de Lille I et du CNRS (UMR 8523). CERLA is Fédération de Recherche du CNRS (FR 2416).

[1] F. Gires and F. Combaud, *J. Phys. (Paris)* **26**, 325 (1965).
 [2] V. E. Kartsiev, D. I. Stasel’ko, and V. M. Ovchinnikov, *Sov. Phys. JETP* **25**, 965 (1967).
 [3] A. C. Selden, *Br. J. Appl. Phys.* **18**, 743 (1967).
 [4] A. C. Selden, *J. Phys. D* **3**, 1935 (1970).
 [5] A. C. Selden, *IEEE J. Quantum Electron.* **5**, 523 (1969).
 [6] A. C. Selden, *Electron. Lett.* **7**, 287 (1971).
 [7] L. W. Hillman, R. W. Boyd, J. Krasinski, and C. R. Stroud, *Opt. Commun.* **45**, 416 (1983).
 [8] M. S. Bigelow, N. N. Lepeshkin, and R. W. Boyd, *Phys. Rev.*

Lett. **90**, 113903 (2003).
 [9] M. S. Bigelow, N. N. Lepeshkin, and R. W. Boyd, *Science* **301**, 200 (2003).
 [10] M. S. Bigelow, N. N. Lepeshkin, and R. W. Boyd, *J. Phys.: Condens. Matter* **16**, R1321 (2004).
 [11] Y. D. Zhang, B. H. Fan, P. Yuan, and Z. G. Ma, *Chin. Phys. Lett.* **21**, 87 (2004).
 [12] M. S. Bigelow, N. N. Lepeshkin, H. Shin, and R. W. Boyd, *J. Phys.: Condens. Matter* **18**, 3117 (2006).
 [13] E. Baldit, K. Bencheikh, P. Monnier, J. A. Levenson, and V.

- Rouget, Phys. Rev. Lett. **95**, 143601 (2005).
- [14] P. Wu and D. V. G. L. N. Rao, Phys. Rev. Lett. **95**, 253601 (2005).
- [15] C. S. Yelleswarapu, R. Philip, F. J. Aranda, B. R. Kimbal, and D. V. G. L. N. Rao, Opt. Lett. **32**, 1788 (2007).
- [16] P. C. Ku, F. Sedgwick, C. J. Chang-Hasnain, P. Palinginis, T. Li, H. Wang, S. W. Chang, and S. L. Chuang, Opt. Lett. **29**, 2291 (2004).
- [17] J. Mørk, R. Kjør, M. van der Poel, and K. Yvind, Opt. Express **13**, 8136 (2005).
- [18] M. van der Poel, J. Mørk, and J. M. Hvam, Opt. Express **13**, 8032 (2005).
- [19] H. Su and S. L. Chuang, Appl. Phys. Lett. **88**, 061102 (2006).
- [20] P. C. Ku, C. J. Chang-Hasnain, and S. L. Chuang, J. Phys. D **40**, R93 (2007).
- [21] A. Schweinsberg, N. N. Lepeshkin, M. S. Bigelow, R. W. Boyd, and S. Jarabo, Europhys. Lett. **73**, 218 (2006).
- [22] S. Melle, O. G. Calderon, F. Carreno, E. Cabrera, M. A. Anton, and S. Jarabo, Opt. Commun. **279**, 53 (2007).
- [23] S. E. Schwarz and T. Y. Tan, Appl. Phys. Lett. **10**, 4 (1967).
- [24] V. S. Zapasskii and G. G. Kozlov, Opt. Spectrosc. **100**, 419 (2006).
- [25] A. C. Selden, e-print arXiv:physics/0512149.
- [26] V. S. Zapasskii and G. G. Kozlov, Opt. Spectrosc. **104**, 95 (2008).
- [27] Note, however, that the CPO analysis is perfectly applicable to the experiment of P. C. Ku *et al.* [16], where two independent coherent beams are actually used.
- [28] G. Piredda and R. W. Boyd, J. Eur. Opt. Soc. Rapid Publ. **2**, 07004 (2007).
- [29] We use the current definition of the saturation intensity which differs by a factor 2 from that used in the first works [1–5].
- [30] S. Choblet, Ph.D. thesis, Université de Lyon 1, Lyon, 2004.
- [31] Throughout this section we use the definitions, sign conventions and classical results of the signal theory. See, e.g., A. Papoulis, *Signal Analysis* (McGraw-Hill, New York, 1988).
- [32] H. Shin, A. Schweinsberg, G. Gehring, K. Schwertz, H. J. Chang, R. W. Boyd, Q.-H. Park, and D. J. Gauthier, Opt. Lett. **32**, 906 (2007).
- [33] B. Macke and B. Ségard, Phys. Rev. A **73**, 043802 (2006).
- [34] The corresponding peak intensity of the output pulse is $A_{\text{out}} \approx 0.01$. It can be led to 0.05 by taking $\alpha L = 9$ without significant reduction of F_{max} .
- [35] K. Y. Song, M. G. Herráez, and L. Thévenaz, Opt. Lett. **30**, 1782 (2005).
- [36] P. W. Milonni, *Fast Light, Slow Light and Left-Handed Light* (IOP, Bristol, 2005).
- [37] A. Kasapi, M. Jain, G. Y. Yin, and S. E. Harris, Phys. Rev. Lett. **74**, 2447 (1995).
- [38] H. Tanaka, H. Niwa, K. Hayami, S. Furue, K. Nakayama, T. Kohmoto, M. Kunitomo, and Y. Fukuda, Phys. Rev. A **68**, 053801 (2003).
- [39] R. M. Camacho, M. V. Pack, J. C. Howell, A. Schweinsberg, and R. W. Boyd, Phys. Rev. Lett. **98**, 153601 (2007).